# Validation of Cyclic Void Growth Model for Fracture Initiation in the Flange Plate Connection Between Beam and Box Column

**M. Tehranizadeh, A. Deylami, M. Gholami & H. Moazemi**
*Amirkabir University of Technology, Iran*

**SUMMARY**

The flange plate connections show ductile tearing at plastic hinge region. These ductile tears accompanied by large-scale yielding have the potential to transition tocleavage type failure. Consequently, ductile fracture is a governing limit state in the reinforcing plate connections.. In this study, the cyclic void growth model (CVGM) was used to simulate ductile fracture initiation in the flange plate connections. By comparing simulation-based predictions to experimental results the accuracy of CVGM model to predict ductile fracture initiation in the flange plate connections was validated.

*keywords: Connections; Flange Plate; Steel beam;Experimental program; Finite element analysis; Ductile fracture;*

## 1. INTRODUCTION

The Northridge and Kobe earthquakes demonstrated that fracture is an important mode of failure in steelmoment connections during earthquakes. Many experimental studies after the Northridge earthquake, resulted in recommendations for developing fracture-resistant connections (Kim et al, 2002, Ricles et al, 2002, Chen et al, 2005, Tabar et al, 2004, Shiravand et al, 2010, Adeli et al, 2011).. These recommendations included (1) reducing the imposed toughness demands by modifying the connections – e.g. removal of backing bars orminimizing flaws through better quality control during welding (2) using notch-toughness rated materials for base metals as well as weld metals to meet the imposed demands successfully.3) using reinforcing plate such as flange plate, cover plate and rib plate.

However, studies such as Stojadinovic et al. (2000) showed that despite their resistance to brittle fracture, the reinforcing plate connections show ductile tearing at plastic hinge region. These ductile tears accompanied by large-scale yielding have the potential to transition tocleavage type failure.Consequently, ductile fracture is a governing limit state in the reinforcing plate connections. Thus, an accurate prediction of ductile tearing at plastic hinge region is a critical component needed to describe performance of reinforcing plate connections.

Traditional fracture mechanics, including linear elastic approaches like the $K_{IC}$ or elastic-plastic approaches such as the J-integral or the Crack Tip Opening Displacement (CTOD) can predict fracture in situations with limited yielding and the presence of an initial crack, they are of limited use in situations such as reinforcing plate connections, where fracture initiates after widespread yielding without the presence of a sharp crack or flaw (Kanvinde et al., 2006). In this study, the cyclic void growth model (CVGM) was used to simulate ductile fracture initiation in the flange plate connections. This model was developed by Kanvinde et al. (2007a). The CVGM predicates ductile fracture initiation through plastic strain and stress triaxiality histories that can be modeled at the material continuum level by finite-element analyses.

In the present study, the accuracy of CVGM model to predict ductile fracture initiation in the flange plate connections was investigated by comparing simulation-based predictions to experimental results.

## 2. Theory OF CVGM MODEL

This section provides only a brief overview of the CVGM model theory. The theoretical basis for the CVGM and extensive discussion regarding its development is provided in Kanvinde et al. (2007a). Ductile fracture and fatigue in steel is caused by the processes of void nucleation, growth, and coalescence. As steel experiences a state of triaxial stress, voids tend to nucleate and grow around inclusions (mostly carbides in mild steels) in the material matrix and coalesce until a macroscopic crack is formed in the material. Previous research (Rice and Tracy, 1969) has shown that void growth is highly dependent on equivalent plastic strain, $\varepsilon_p$, and stress triaxiality, $T = \frac{\sigma_m}{\sigma_e}$, where $\sigma_m$ is the mean or hydrostatic stress and $\sigma_e$ is the von Mises stress. Cyclic void growth demand, $VGD_{cyclic}$, is calculated by following equation :

$$VGD_{cyclic} = \sum_{tensile-cyclic} \int_{\varepsilon_1}^{\varepsilon_2} \exp(|1.5T|).d\varepsilon_p - \sum_{compressive-cyclic} \int_{\varepsilon_1}^{\varepsilon_2} \exp(|1.5T|).d\varepsilon_p \qquad (2.1)$$

$d\varepsilon_p$=differential increment of the equivalent plastic strain. For ductile fracture to occur, $VGD_{cyclic}$, should exceeds cyclic void growth capacity, $VGC_{cyclic}$. The cyclic void growth capacity, $VGC_{cyclic}$, is defined by following equation:

$$VGC_{cyclic} = \beta.\exp \quad (-\alpha.\varepsilon_p^{accumulated}) \qquad (2.2)$$

Where $\beta$ , $\alpha$ =material parameter, and $\varepsilon_p^{accumulated}$ is defined as the equivalent plastic strain that has accumulated up to the beginning of each "tensile" excursion of loading and its value remains constant within each tensile excursion. Thus, when applying the CVGM criterion, $\varepsilon_p^{accumulated}$ is calculated at the beginning of each tensile excursion for a given material point, and substituted into Eqn. 2.2 to determine the current cyclic void growth capacity, $VGC_{cyclic}$. Fracture index (FI) can now be defined at any point in the loading history (Kanvinde et al., 2007a) :
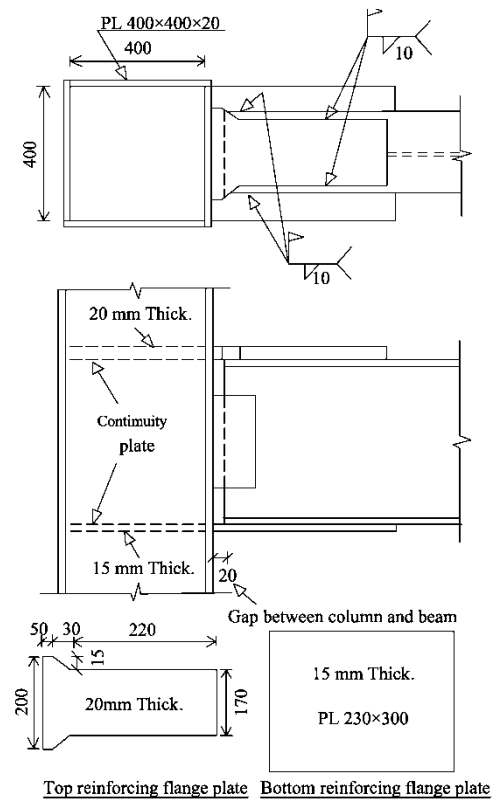
$$FI = \frac{VGD_{cyclic}}{VGC_{cyclic}} \qquad (2.3)$$

This quantity represents a limit state at a single point which expresses how close the material is to ductile crack initiation. Thus, a low index would suggest that the material is safe from fracture, while an index closer to unity indicates a higher probability of ductile fracture at that point.

## 3. EXPRIMENTAL PROGRAM

Gholami et al. (2012) tested two full scale flange plate connection. Both the test specimens were constructed with a I-380 ×200 ×8 ×12 (mm) beam and a built-up B-400 × 400 × 20 × 20 (mm) box column, to reduce the influence of the size of the beam and the column on the connection behavior. Beams, columns and the other connection plates were all A36 steel. The specimens were named as LF30 and LF50. Fig. 1 shows connection details of specimen LF30. Specimen LF50 was identical to LF30 except that the flange-plate length was increased from 300 to 500 mm.
The general configuration of the test setup is shown in Fig. 5. The column top and bottom were supported by real hinges. The beam was laterally braced in the vicinity of the plastic hinge and also near the beam end. The cyclic displacement proposed by AISC seismic provisions was applied at the tip of the beam by a hydraulic actuator.

**Figure 1.** Connection details of specimen LF30



**Figure 2.** Test setup configuration

Both the test specimens achieved the AISC seismic provision requirements for special moment frames. Fig.3 shows the test specimens LF30 and LF50-T at 5% rad story drift angle. In the test specimens, plastic hinge forms in the beam at the nose of flange plate. Such a result is desirable because the objective of the flange-plate connection is to force inelastic action in the beam away from the column face.

In the specimen LF50, tearing was occurred at the groove weld joining the beam web to the beam flange in the plastic hinge region, as shown in Fig. 1. In contrast, no crack was observed in the specimen LF30. This indicates that a longer flange plate increases potential for fracture at the plastic hinge region.



a)



b)

**Figure 3.** Test specimens at the end of the test a) LF30 b) LF50
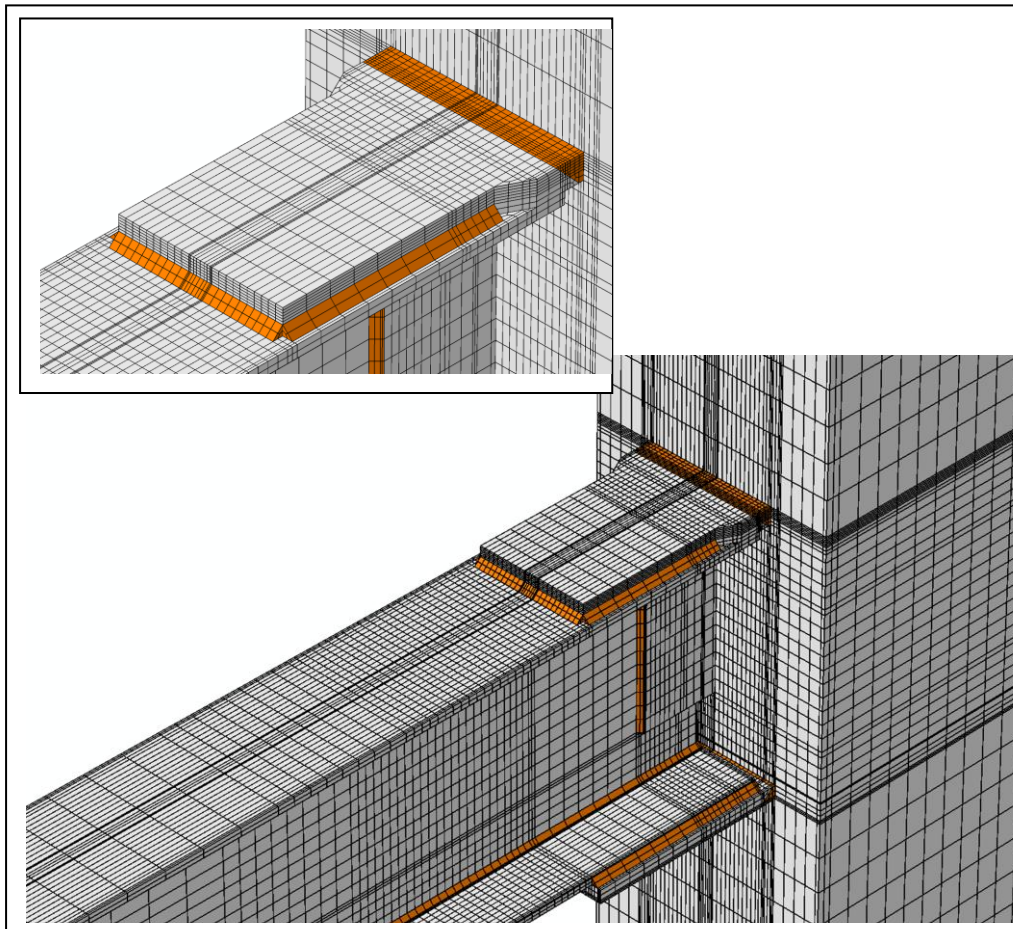
## 4. NONLINEAR FINITE-ELEMENT ANALYSIS

### 4.1. Finite element modeling

ABAQUS models of LF30 and LF50 were prepared. As shown in Fig. 4, groove welds and fillet welds were modeled. The beam, column, plates, CJP groove welds and fillet welds in the model were discretized using three-dimensional solid (brick) elements. The size of the finite-element mesh varied over the length and height of the model. A fine- mesh was used near the connection of the beam to the column and the beam flange to the reinforcing plate. A coarser mesh was used elsewhere. Most of the solid elements were right-angle prisms. Hinged boundary conditions were used to support the column top and bottom. The load was applied by imposing incremental vertical displacements at the beam tip during the analysis.

Data from tests of coupons extracted from the beam and column of specimen were used to establish the stress-strain relationships for the beam and column elements. The weld material was modeled using the test data of Kaufmann (1976). Table 4.1 presents the material properties used for the analytical models. A bilinear stress-strain relationship was assumed for each of the components identified in Table 4.1. The Poisson's ratio was taken as 0.3 for all materials throughout the analyses. To account for material nonlinearities, the von mises yield criterion was employed. Table 4.2 presents the material properties used for the CVGM model, $\alpha$ and $\beta$. these material properties were obtained using the test data of Kanvinde et al. (2007b). A FORTRAN subroutine was prepared that links with ABAQUS/Standard and calculates Rupture index, allowing its contour to be plotted with the visualization software in ABAQUS.



**Figure 4.** Finite element model

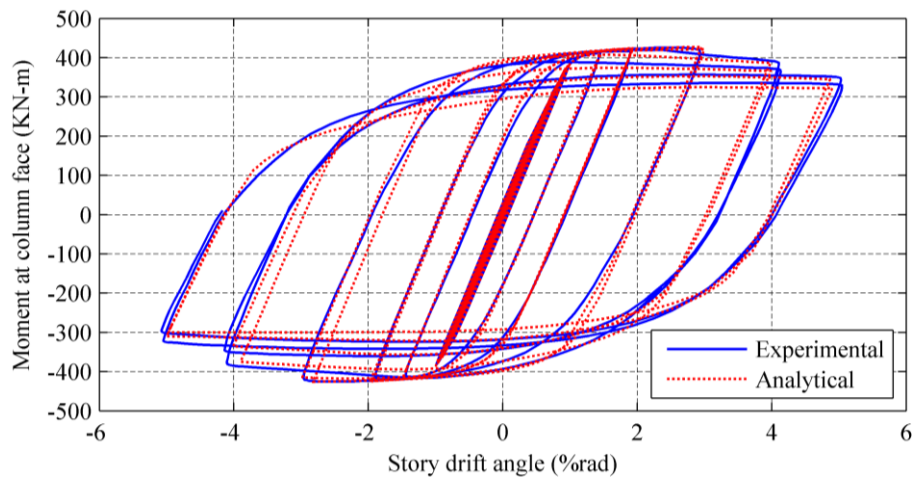**Table 4.1**. Material properties used for the analytical models

| Component | Yield point | | Ultimate point | |
|---|---|---|---|---|
| | Stress (Mpa) $\sigma_y$ | Strain (%) $\varepsilon_y$ | Stress (Mpa) $\sigma_u$ | Strain (%) $\varepsilon_u$ |
| Beam flange | 3050 | 0.15 | 4200 | 18 |
| Beam web | 2900 | 0.145 | 4100 | 18 |
| Column flange | 2700 | 0.135 | 3650 | 15 |
| Column web | 2700 | 0.125 | 3650 | 14 |
| Reinforcing plates | 2650 | 0.1225 | 3600 | 15 |
| Continuity plates | 2650 | 0.1275 | 3700 | 15 |
| Weld material | 5250 | 0.26 | 5600 | 12 |

**Table 4.2**. Material properties used for the CVGM model

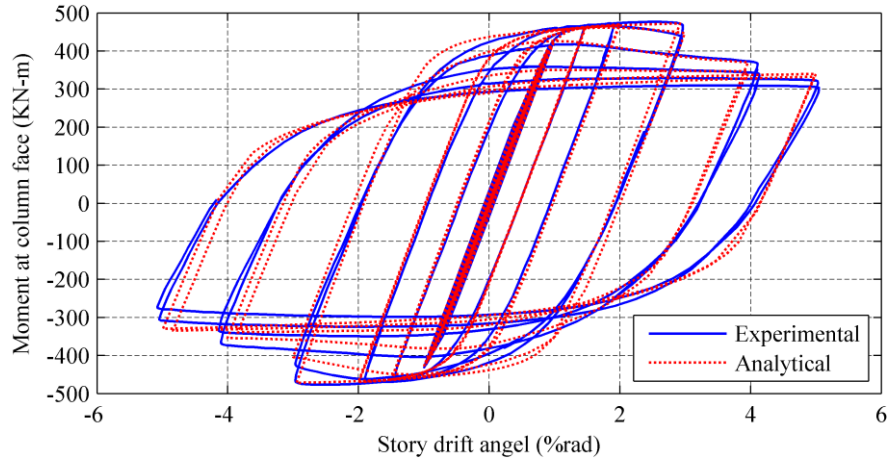| Material | $\alpha$ | $\beta$ |
|---|---|---|
| Steel | 1 | 2.5 |
| Weld | .5 | 1.2 |

## 4.2. Model validation

The finite element analysis of specimens LF30 and LF50 were performed. The cyclic outcomes are compared with the cyclic experimental results, as shown in Fig. 5. The experimental and finite element results are in good agreement. While the ultimate load and initial stiffness are well evaluated, the extant differences between the two data sets are justified by geometric differences between the finite element models and specimens, uncertainties in the material model, and also unavoidableresidual stresses.
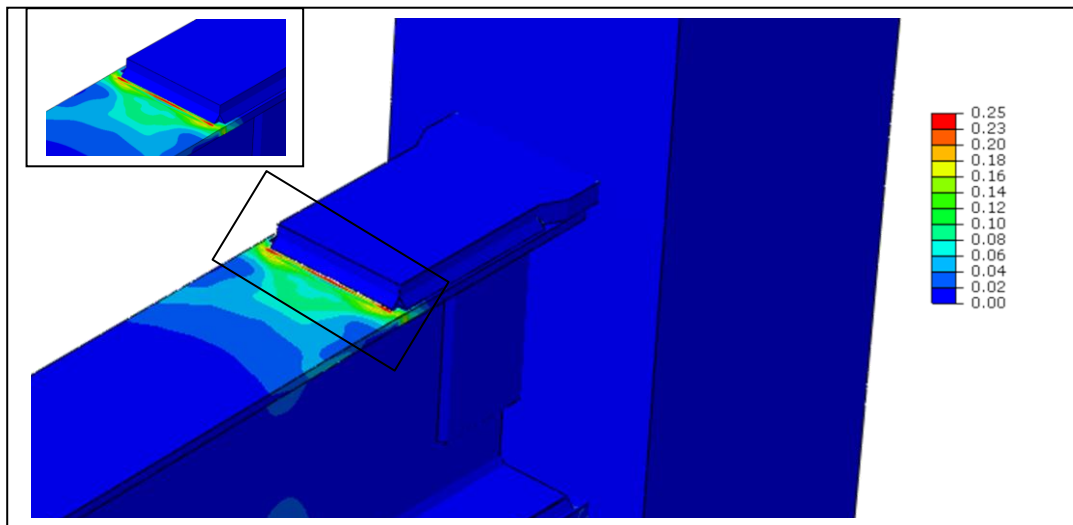


a)

b)

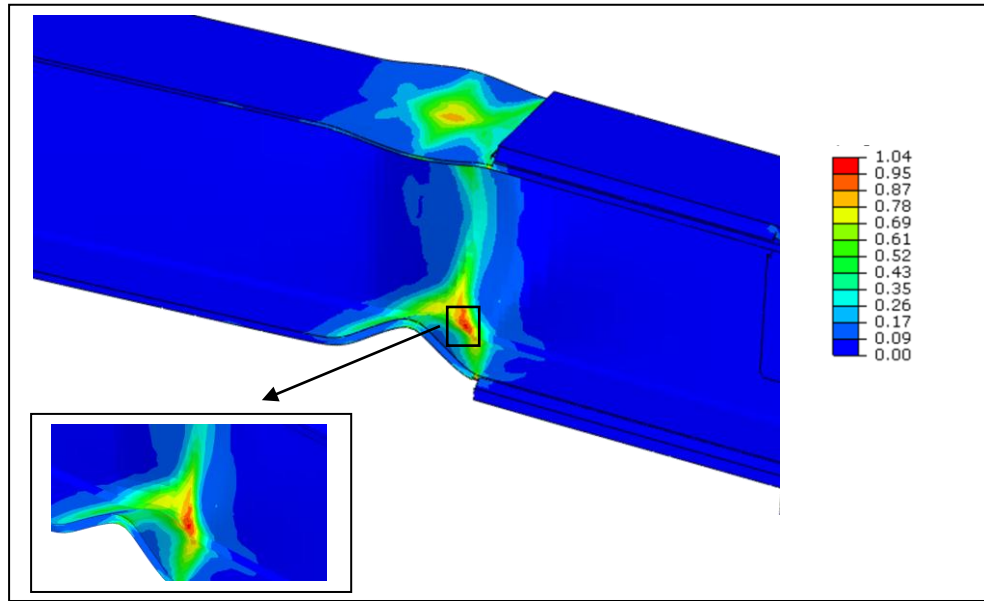**Figure 5.** Combined plot of experimental and analytical results for specimens a) LF30 and b) LF50

## 4.3. Validation of CVGM model

By comparing simulation-based predictions to experimental results the accuracy of CVGM model to predict ductile fracture initiation in the flange plate connections was validated. Fig. 6 presents the RI contours in the finite element model LF30 at 3% rad story drift angle. The RI contours of specimen LF50 was similar to that of specimen LF30 at 3% rad story drift angle. The maximum value of the RI in the models LF50 and LF30 is approximately 0.25 and was occured in the beam at the nose of flange plate. This indicates that models are safe from ductile fracture initiation, untile 3% rad story drift angle. Because the maximum value of RI for models is sustantioly less than unity.
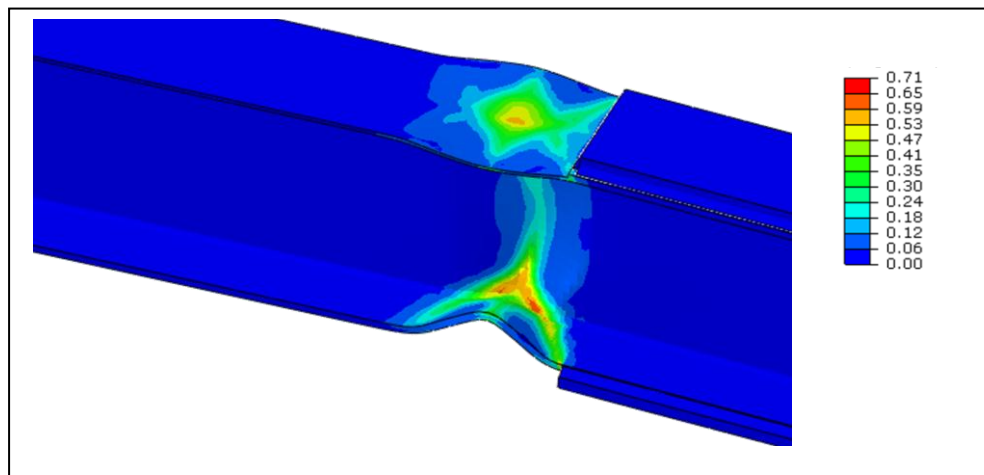
Fig. 7 presents the RI contours in the finite element models LF30 and LF50 at 5% rad story drift angle. It is apparent from the contour plot shown in Fig. 4 that the groove weld joining the beam web to the beam flange at the plastic hinge region of model is the critical location and will be the location of ductile fracture initiation. Comparing this location to the experimental fracture location (as shown in the figure) demonstrates the accuracy of the CVGM model to predict ductile fracture initiation in the flange plate connections.



**Figure 6.** RI contours in the finite element model LF30 at 3% rad story drift angle

a)



b)

**Figure 7.** RI contours in the finite element models a) LF30 and b) LF50 at 5% rad story drift angle.

## 5. CONCLUSIONS

In this study, the cyclic void growth model (CVGM) was used to simulate ductile fracture initiation in the flange plate connections. By comparing simulation-based predictions to experimental results the accuracy of CVGM model to predict ductile fracture initiation in the flange plate connections was validated.

**REFERENCES**

Nakashima, M., Roeder, CW. and Maruoka, Y. (2000). Steel moment frames for earthquakes in United States and Japan. *J Struct Eng* **126:8**, 861–8.

Kim T., Whittaker AS., Gilani ASJ., Bertero, VV. and Takhirov, SM. (2002). Cover-plate and flange-plate steel moment-resisting connections. *Journal of Structural Engineering* **128:4**, 474–482.

Ricles, JM., Fisher, JW., Lu LW. and Kaufmann, EJ. (2002). Development of improved welded moment connections for earthquake-resistant design. *Journal of Constructional Steel Research* **58:4**, 565–604.

Chen, C., Chen, SW., Chung, MD. and Lin, MC. ( 2005). Cyclic behavior of unreinforced and rib-reinforced moment connections. *Journal of Constructional Steel Research* **61:6**, 1–21.

Tabar, A.M. and Deylami, A. (2004). Investigation of major parameters affecting instability of steel beams with RBS moment connections. *Steel and Composite Structures* **6:3**, 1475-1491.

Shiravand, M. and Deylami, A. (2010). Application of Full Depth Side Plate to Moment Connection of I-Beam to Double-I Column. *Advances in Structural Engineering* **13:6**, 1047-1062.

Adeli, M., Banazadeh, M. and Deylami, A. (2011). Bayesian approach for determination of drift hazard curves for generic steel moment-resisting frames in territory of Tehran. *International Journal of Civil Engineering* **9: 3**, 145-154.

Stojadinovic, B., Goel, S., and Lee, K.H. (2006). Development of post-Northridge steel moment Connections. *Proceedings of the12th World Conference on Earthquake Engineering, New Zealand, paper*

Kanvinde, AM. and Deierlein, GG. (2006). The void growth model and the stress modified critical strain model to predict ductile fracture in structural steels. *J. Struct. Eng*. **132:12**, 1907–1918.

Kanvinde, AM. and Deierlein, GG. (2007). Cyclic void growth model to assess ductile fracture initiation in structural steels due to ultra low cycle fatigue. *J. Eng. Mech*. **133:6**, 701–712.

Kanvinde, AM. and Deierlein, GG.(2007). Finite-element simulation of ductile fracture in reduced section pull plates using micromechanics fracture models. *J. Struct. Eng*. **133:5**, 656–664.

Rice, JR. and Tracey, DM. (1969). On the ductile enlargement of voids in triaxial stress fields. *J. Mech. Phys. Solids*. **35:9**, 201–217.

Gholami, m., Tehranizadeh, M. and Deylami, A. (2012). Behaviore of flange plate connections between steel beam and box column. *Advance steel constraction* **11:3**, 1017-1032.

Kaufmann, EJ. (1997). Dynamic tension tests of simulated moment resisting frame weld joints.Chicago. Steel Tips, Structural Steel Education Council. *American Institute of Steel Construction* .